A Periodogram-Based Method for the Detection of Steady-State Visually Evoked Potentials

Athanasios P. Liavas,* George V. Moustakides, *Senior Member, IEEE*,
Günter Henning, Emmanuil Z. Psarakis, and Peter Husar

***Abstract*—The task of objective perimetry is to scan the visual field and find an answer about the function of the visual system. Flicker-burst stimulation—a physiological sensible combination of transient and steady-state stimulation—is used to generate deterministic sinusoidal responses or visually evoked potentials (VEP's) at the visual cortex, which are derived from the electroencephalogram by a suitable electrode array. In this paper we develop a new method for the detection of VEP's. Based on the periodogram of a time-series, we test the data for the presence of hidden periodic components, which correspond to steady-state VEP's. The method is applied successfully to real data.**

***Index Terms*— Hidden periodicities, periodogram, visually-evoked potentials.**

I. Introduction

THE part of the visual world which can be seen by an eye is called monocular visual field. A defect of this field can be caused either by deterioration of the retina, the visual pathway, or the visual cortex. Perimetry is a method to discover these defects. The examination of the visual field is currently carried out by subjective methods. Such techniques require the assistance of patients, thus, they are not feasible in cases of infants, simulants, and critically ill patients.

The objective perimetry is based on the analysis of visual evoked responses [1]. In the ophthalmologic diagnostics, well-defined light stimuli are used for stimulating the visual system. These stimuli elicit responses in the visual cortex, which are acquired as visually evoked potentials (VEP's) by means of a suitable system of electrodes. After a proper signal processing and the quantification of the VEP parameters, these can be utilized for objectifying diagnostics. In case of well-defined diagnostic questions (determination of the visual field) it is necessary to find out, with sufficient reliability, whether a VEP is present or not. From the point of view of signal processing, the task is to detect a signal (VEP) in the biological noise [spontaneous electroencephalogram (EEG)].

Depending on the stimulation frequency a distinction is made between transient VEP (tVEP) and steady-state VEP (ssVEP). Transient VEP's arise if the electrical excitations of the visual system are able to abate before new stimuli are presented. If the repetition rate of stimuli is faster than 6/s, responses begin to merge and the shape of the resulting ssVEP becomes periodic. The detection problem then is reduced to find this periodic component in the spontaneous EEG.

In our experiment, we combine both steady-state and transient stimulation methods to a flicker-burst stimulation. A tracing of 4 s (prestimulus data) is followed by a 4-s burst of flicker stimuli (post-stimulus data) in which the basic stimulation frequency is selected to be 8 Hz. Thus, the first and second harmonics have a sufficient distance from the α-band.

A wide range of approaches to the detection of ssVEP's have been proposed with the most recent ones including, among many others, classical frequency-domain approaches [2], adaptive matched filtering [3], and time-frequency analysis [4].

In this paper, we develop a new method for the detection of ssVEP's based on the periodogram. We test the post-stimulus data for the presence of hidden periodic components, which correspond to the ssVEP's. In Section II, we develop the statistical test for the presence of hidden periodicities; in Section III, we apply this test for the detection of ssVEP's; in Section IV, we compute the power of the statistical test; in Section V, we present results of the application of this statistical test on real data. Conclusions are drawn is Section VI.

II. Test for the Presence of Hidden Periodicities

In this section, we develop a statistical test for testing the data for the presence of hidden periodic components; the test is based on the periodogram of a time-series.

In the sequel, we provide the definition of the periodogram, as well as its properties related to the construction of the statistical test. We represent stochastic quantities with bold letters.

A. Periodogram

The periodogram of a time-series $\{\boldsymbol{y}(n), n = 1, \cdots, N\}$ is defined as in [5, p. 331]

$$\boldsymbol{I}_y(\omega_k) = \frac{1}{N}\left|\sum_{n=1}^{N} \boldsymbol{y}(n) e^{-j\omega_k n}\right|^2 \tag{1}$$

with $\omega_k = 2\pi k/N$, $k = 1, \cdots, N$. Periodogram ordinates are symmetric around $N/2$, assuming N even, i.e., $\boldsymbol{I}_y(\omega_k) =$

Manuscript received April 15, 1996; revised July 2, 1997. *Asterisk indicates corresponding author.*

*A. P. Liavas is with the Départment SIM, Institut National des Télécommunications, 9 rue Charles Fourier, 91011 Evry Cedex, France (e-mail: liavas@pollux.int-evry.fr).

G. V. Moustakides and E. Z. Psarakis are with the Department of Computer Engineering and Informatics, University of Patras, 26500 Patras, Greece.

G. Henning and P. Husar are with the Department of Biomedical Engineering and Medical Informatics, Technical University Ilmenau, PSF 327, D-98684 Ilmenau, Germany.

Publisher Item Identifier S 0018-9294(98)00917-3.

$\boldsymbol{I}_y(\omega_{N-k})$. The value $\boldsymbol{I}_y(\omega_k)$ is a measure of the energy contribution of the frequency ω_k to the "signal effect" [6, p. 24].

If $\{\boldsymbol{y}(n),\ n = 1, \cdots, N\}$ are samples of a stationary time-series with autocorrelation sequence $\{r_y(i), -\infty < i < \infty\}$, then periodogram ordinates, $\boldsymbol{I}_y(\omega_k)$, are *asymptotically independent exponential* random variables, with mean $S_y(\omega_k)$ [5, p. 330]. The function $S_y(\omega)$ is the power spectral density (psd) of $\{\boldsymbol{y}(n)\}$ and is given by the Fourier transform of the autocorrelation sequence $\{r_y(i)\}$. Notice that the psd is a deterministic function of ω.

In the sequel, we assume that N is large enough so that we may regard periodogram ordinates as independent exponential random variables [5, p. 342]. Thus, the probability density function (pdf) of the random variable $\boldsymbol{I}_y(\omega_k)$ can be expressed as

$$P_{\boldsymbol{I}_{y(\omega_k)}}(a) = \begin{cases} \frac{1}{S_y(\omega_k)}\, e^{-a/S_y(\omega_k)}, & a \geq 0, \\ 0, & \text{otherwise.} \end{cases} \tag{2}$$

Equivalently, we can say that the random variable $\boldsymbol{I}_y(\omega_k)/S_y(\omega_k)$ is distributed according to the $\chi^2(2)/2$ distribution, where $\chi^2(2)$ is the chi-square distribution with two degrees of freedom, i.e.,

$$\frac{\boldsymbol{I}_y(\omega_k)}{S_y(\omega_k)} \sim \frac{1}{2}\,\chi^2(2). \tag{3}$$

If $\boldsymbol{z} \sim \chi^2(k)$, $\boldsymbol{w} \sim \chi^2(r)$, and $\boldsymbol{z}$, $\boldsymbol{w}$ independent, then [7, pp. 219–223]

$$(\boldsymbol{z} + \boldsymbol{w}) \sim \chi^2(k + r) \tag{4}$$

$$\frac{\boldsymbol{z}/k}{\boldsymbol{w}/r} \sim F(k, r) \tag{5}$$

where $F(k, r)$ is the F-distribution with k and r degrees of freedom.

Properties (3)–(5) and the (asymptotic) independence of the periodogram ordinates will be the main tools for the construction of the statistical test presented in the next subsection.

B. Test for the Presence of Periodic Components of Specified Basic Frequency

Let us assume that we are given a set of data $\{\boldsymbol{x}(1), \cdots, \boldsymbol{x}(N)\}$. In this subsection, we develop a statistical test based on the periodogram, which can be used to test the null hypothesis, that the data are samples of a stationary time-series, against the alternative hypothesis, that the data are samples of a stationary time-series with a superimposed periodic component of known basic frequency. More specifically, let us assume that $f(n)$ is a periodic signal of the form

$$f(n) = \sum_{i=1}^{m} A_i \cos(i\omega_0 n) + B_i \sin(i\omega_0 n), \quad n = 1, \cdots, N \tag{6}$$

where ω_0 is the specified basic frequency, and A_i, B_i, $i = 1, \cdots, m$, are *nonrandom*, but *unknown* constants. An additional assumption is that $\omega_0 = 2\pi m_0/N$, for some integer m_0 between 1 and $[N/(2m)]$, where $[x]$ denotes the integer part of x. In this way, we avoid aliasing and we simplify the analysis since the periodogram at $i\omega_0$ is directly computed via (1), i.e., $i\omega_0$, $i = 1, \cdots, m$, belong to the set of the so-called Fourier frequencies, $\omega_k = 2\pi k/N$, $k = 1, \cdots, N/2$, [5, p. 331]. Our data model is

$$\boldsymbol{x}(n) = f(n) + \boldsymbol{y}(n), \quad n = 1, \cdots, N \tag{7}$$

where $\boldsymbol{y}(n)$ is a stationary time-series with psd $S_y(\omega)$.

The null and the alternative hypotheses are

$$H_0\text{: } A_i = B_i = 0, \qquad \text{for all}$$
$$H_1\text{: } H_0 \text{ is false.}$$

Let us assume that $S_y(\omega)$ is known to within a scaling factor, i.e.,

$$S_y(\omega) = \sigma \hat{S}_y(\omega) \tag{8}$$

where $\hat{S}_y(\omega)$ is known and σ is considered unknown.

We observe that under H_0, $\boldsymbol{x}(n) = \boldsymbol{y}(n)$, $n = 1, \cdots, N$, which means that $\boldsymbol{I}_x(\omega_k) = \boldsymbol{I}_y(\omega_k)$, $k = 1, \cdots, N$. Using (3) and (8), we obtain that under H_0

$$\frac{\boldsymbol{I}_x(\omega_k)}{\hat{S}_y(\omega_k)} \sim \frac{\sigma}{2}\,\chi^2(2). \tag{9}$$

On the other hand, under H_1, $\boldsymbol{I}_x(i\omega_0)$ will differ from $\boldsymbol{I}_y(i\omega_0)$, for some i, depending on which A_i, B_i differ from zero. At the frequencies $i\omega_0$, where there is a difference between $\boldsymbol{I}_x(i\omega_0)$ and $\boldsymbol{I}_y(i\omega_0)$, we expect that $\boldsymbol{I}_x(i\omega_0)$ will be larger than $\boldsymbol{I}_y(i\omega_0)$, due to the power of the superimposed sinusoids. Thus, we expect that

$$\frac{\boldsymbol{I}_x(i\omega_0)}{\hat{S}_y(i\omega_0)} \succ \frac{\sigma}{2}\chi^2(2) \tag{10}$$

with "$\succ$" meaning that the random variable at the left-hand side takes, with high enough probability, larger values than the values usually obtained by a random variable distributed as a $(\sigma/2)\chi^2(2)$.

Based on these observations, we reject H_0 in favor of H_1, if $\sum_{i=1}^{m} \boldsymbol{I}_x(i\omega_0)/\hat{S}_y(i\omega_0)$ is sufficiently large. In order to put this statement under a statistical test, let us recall the (asymptotic) independence of the periodogram ordinates and (3), (4), and (8). Then, under H_0, we have

$$\mathcal{A}_1 = \sum_{i=1}^{m} \frac{\boldsymbol{I}_x(i\omega_0)}{\hat{S}_y(i\omega_0)} \sim \frac{\sigma}{2}\chi^2(2m) \tag{11}$$

$$\mathcal{A}_2 = \sum_{\substack{\omega_k \in \Omega \\ \omega_k \neq i\omega_0,\ i=1,\cdots,m}} \frac{\boldsymbol{I}_x(\omega_k)}{\hat{S}_y(\omega_k)} \sim \frac{\sigma}{2}\,\chi^2(2M) \tag{12}$$

where Ω is a frequency window containing the M frequency bins which we select to use in our test. Ω can be constructed in various ways, depending on *a priori* knowledge concerning the properties of the signals over different frequency bands. (We have to say more about the construction of Ω in Section III, where we apply the test to real data.)

Since $\mathcal{A}_1$ and $\mathcal{A}_2$ refer to nonoverlapping Fourier frequencies, they are independent random variables. Thus, using (5) we have that under H_0

$$\mathcal{A} = \frac{\mathcal{A}_1/2m}{\mathcal{A}_2/2M} \sim F(2m, 2M). \tag{13}$$

Consequently, we reject H_0 in favor of H_1 at level a if

$$\mathcal{A} > F_{1-a}(2m, 2M). \tag{14}$$

III. Detection of ssVEPs

In this section, we use the statistical test presented in the previous subsection for the detection of ssVEP's.

The ssVEP's are generated by a sequence of green bright LED flashes with frequency 8 Hz ($L = 20 \cdots 40 \times 10^4$ cd/m^2; $\lambda = 560$ nm). The stimulus size of the local stimulation is about $1y$ of the visual angle. To elicit visually evoked responses, the EEG is recorded using 16 electrodes placed over the visual cortex. The distance between the electrodes is set to be 10% of the distance nasion-inion. The arithmetic mean of the left and right ear potential is used as reference level. After amplification and filtering (bandpass 0.3–40 Hz Bessel-characteristic second order), the EEG data are sampled at 250 Hz and A/D converted (12 bit). The amplitudes of ssVEP's (10 μV) are normally below the amplitudes of an EEG signal (100 μV).

A. Data Models

For each stimulated eye position, we derive one time-series by time averaging over 32 realizations of the data derived from the channel Oz-AVO. Each resulting time-series is composed of two parts:

- 1000 samples of pure EEG data recorded just before the stimulation begun (prestimulus signal);
- 1000 samples of EEG plus stimulation response data recorded just after stimulation begun (post-stimulus signal).

As we have already mentioned, if the repetition rate of the stimuli is larger than 6/s, responses begin to merge and the shape of the resulting ssVEP becomes periodic. Thus, the data models for the pre- and post-stimulus signals can be respectively expressed, for $n = 1, \cdots, 1000$, as

$$\boldsymbol{x}_{\rm pre}(n) = \boldsymbol{y}_{\rm pre}(n) \tag{15}$$

$$\boldsymbol{x}_{\rm post}(n) = \sum_{i=1}^{m} A_i \cos(i\omega_0 n) + B_i \sin(i\omega_0 n) + \boldsymbol{y}_{\rm post}(n) \tag{16}$$

where m is the number of harmonics we are trying to detect, A_i, B_i, and $i = 1, \cdots, m$, are nonrandom but unknown numbers, and $\omega_0 = 2\pi$ (8/250) is the basic frequency, because the basic stimulation frequency is 8 Hz and the sampling frequency is 250 Hz. The time-series $\boldsymbol{y}_{\rm pre}(n)$ and $\boldsymbol{y}_{\rm post}(n)$ represent the pure EEG signal in the pre- and post-stimulus data, respectively.

If the EEG is assumed to be a stationary signal, then the time-series $\boldsymbol{y}_{\rm pre}(n)$, $\boldsymbol{y}_{\rm post}(n)$ can be considered as parts of the same stationary process, implying that their psd's, denoted by $S_{y\rm pre}(\omega)$ and $S_{y\rm post}(\omega)$, respectively, coincide. In the sequel, we make a slightly less restrictive assumption, which gives us the ability to handle a special type of nonstationarity. More specifically, we assume that $S_{y\rm pre}(\omega)$ and $S_{y\rm post}(\omega)$ are connected via a scaling factor, i.e.,

$$S_{y\rm post}(\omega) = \sigma S_{y\rm pre}(\omega). \tag{17}$$

This means that the psd's of $\boldsymbol{y}_{\rm post}(n)$ and $\boldsymbol{y}_{\rm pre}(n)$ have the same shape, but not necessarily the same amplitude. It is well known that the EEG signal is nonstationary, especially over certain frequency ranges, for example, over the so-called α-band. However, at frequencies higher than the α-band we do not expect wild nonstationarities. Thus, the assumption of the aforementioned special type of nonstationarity, which includes stationarity, over this frequency range, appears to be reasonable. At this point, the similarity between our hypothetical data model of (7) and our post-stimulus data model of (16) is obvious.

B. Detection of ssVEP's Using the Test for the Presence of Hidden Periodicities

In the sequel, we will use the statistical test derived in the Section II in order to test the post-stimulus data for the presence of hidden periodicities, which correspond to ssVEP's.

In this case $\boldsymbol{I}_x(\omega_k)$ in (11) and (12), must be replaced by $\boldsymbol{I}_{x\rm post}(\omega_k)$, which can be computed via (1).

The next step is to estimate $S_{y\rm post}(\omega)$, which takes the place of $S_y(\omega)$. Notice that the presence of $S_y(\omega)$ in (11) and (12) is implicitly expressed through $\hat{S}_y(\omega)$.

The most natural way to estimate $S_{y\rm post}(\omega)$ is through the post-stimulus data, $\boldsymbol{x}_{\rm post}(n)$. However, since $\boldsymbol{x}_{\rm post}(n)$ contain both EEG and stimulation response, its spectrum around the harmonics of the basic stimulation frequency differs from $S_{y\rm post}(\omega)$, due to the contribution of the stimulation response. This indicates the need of using interpolation techniques to estimate $S_{y\rm post}(\omega)$ at these frequencies. An alternative way is to estimate $S_{y\rm post}(\omega)$ through the prestimulus data. In this way we compute $S_{y\rm pre}(\omega)$, which, as we have already assumed in (17), is connected to $S_{y\rm post}(\omega)$ via the scaling factor σ. Thus, $S_{y\rm pre}(\omega_k)$ takes the place of $\hat{S}_y(\omega_k)$ in (11) and (12).

There are several methods available for computing $S_{y\rm pre}(\omega)$. We select the smoothed periodogram as a robust and reliable method for the construction of a consistent estimate of $S_{y\rm pre}(\omega)$. We use the prestimulus data, $\boldsymbol{x}_{\rm pre}(n)$, which are identical to $\boldsymbol{y}_{\rm pre}(n)$, and we compute $S_{y\rm pre}(\omega)$. Following [6, pp. 153–154] we have

$$S_{y\rm pre}(\omega) = \sum_{\tau=-M}^{M} w(\tau)\hat{R}_y(\tau)e^{-i\tau\omega} \tag{18}$$

where

$$\hat{R}_y(\tau) = \tfrac{1}{1000} \sum_{t=1}^{1000} \boldsymbol{x}_{\rm pre}(n)\boldsymbol{x}_{\rm pre}(n-\tau) \qquad (19)$$

is an estimate of the autocorrelation sequence of the prestimulus EEG signal (values outside the range 1, $\cdots$, 1000, are derived by periodic continuation of $\boldsymbol{x}_{\rm pre}(n)$), $w(\tau)$ is the Hamming lag window

$$w(\tau) = \frac{1}{2}\left(1 + \cos\frac{\pi\tau}{M}\right), \qquad \text{for } 0 \le |\tau| \le M \qquad (20)$$

and $M \ll N$ (typically $M = N/10$).

After the computation of $\boldsymbol{I}_{x\rm post}(\omega_k)$ and $S_{y\rm pre}(\omega_k)$, we may construct $\boldsymbol{I}_{x\rm post}(\omega_k)/S_{y\rm pre}(\omega_k)$, $k = 1, \cdots, N$, and apply the statistical test (14). Of course, it is implied that the number of data samples, i.e., 1000, is large enough, so that we can regard the periodogram ordinates, $\boldsymbol{I}_{x\rm post}(\omega_k)$, as independent exponential random variables.

At this point, some comments on the construction of Ω are in order. Our basic assumption is that the EEG signal is stationary or it exhibits the special type of nonstationarity given in (17). Thus, it is obvious that our test will give more reliable results if we process the frequency intervals in which the EEG possesses these properties. For example, we may *a priori* exclude from Ω the frequency bins over the range 10–14 Hz, where it is possible to encounter wild α-band nonstationarities. However, we must say that even if we encounter wild nonstationarities over certain frequency ranges, their influence on $\mathcal{A}$ will be reduced by the averaging $\mathcal{A}_2/2M$, which takes place in (13). We may also say, that if we are looking for the first harmonics of the basic stimulation frequency, it is not necessary to include in Ω all the frequency bins from 0 to $F_s/2$, where F_s is the sampling frequency. For example, if we are looking for the first 4 harmonics of 8 Hz, we may use the frequency bins from 0 to 40 Hz.

Remark 1: From a signal processing point of view, $\boldsymbol{I}_{x\rm post}(\omega_k)/S_{y\rm pre}(\omega_k)$ is the periodogram of the prewhitened post-stimulus data, using for prewhitening the prestimulus data.

Remark 2: From a Statistics point of view, division of $\boldsymbol{I}_{x\rm post}(\omega_k)$ by $S_{y\rm pre}(\omega_k)$, $k = 1, \cdots, N/2$, is an effort for transforming the random sequence $\boldsymbol{I}_{x\rm post}(\omega_k)$ into a sequence of $(\sigma/2)\chi^2(2)$-distributed random variables. If we observe large peaks in the sequence $\boldsymbol{I}_{x\rm post}(\omega_k)/S_{y\rm pre}(\omega_k)$, then we suspect that something "abnormal" happens, i.e., sinusoidal components are hidden in the stationary time-series at the peak locations.

Remark 3: In order to be able to detect stimulation responses we must detect peaks, at the frequencies $i\omega_0$, in the sequence $\boldsymbol{I}_{x\rm post}(\omega_k)/S_{y\rm pre}(\omega_k)$. This sequence expresses in a way the "change" of the frequency contents of the signal between the post- and prestimulus parts. Test (14) is the statistical rule for detecting a stimulation response, while Remarks 1 and 2 give the physical insight to our detection mechanism. Specifically, for detection we require "*a larger mean increase (smaller mean decrease) of the post-stimulus over the prestimulus psd's at specified frequencies, compared to the corresponding mean increase (decrease) at the neighboring frequencies.*" The quantity $\mathcal{A}_1$ expresses the mean change, increase or decrease, of the frequency content of the signal, between the pre- and post-stimulus parts, at $i\omega_0$ $i = 1, \cdots, m$. On the other hand, $\mathcal{A}_2$ expresses the respective mean change over the neighboring frequencies. Since σ is considered unknown, we cannot make any inference for the presence of periodic components using as a test statistic the value of $\mathcal{A}_1$. However, we may decide via $\mathcal{A}$ since σ is eliminated in (14).

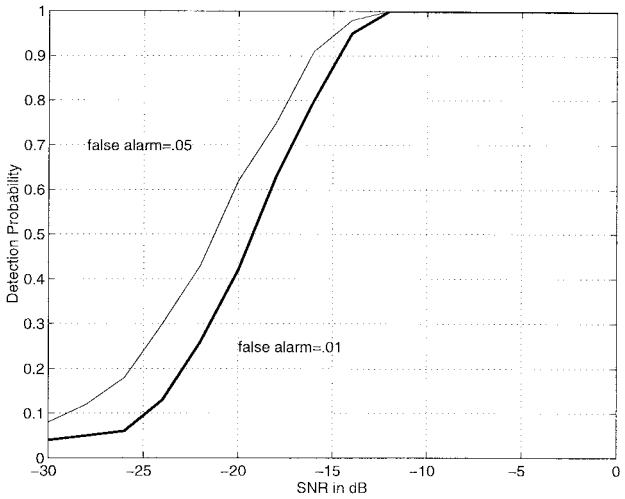

Fig. 1. Power of the periodogram-based detector; $m = 4$, $N = 1000$, false-alarm probability $\alpha = 0.01, 0.05$.

Remark 4: We use the independence and the special type of EEG signal nonstationarity assumptions, in order to be able to derive closed form expressions for the pdf's of the various quantities of interest. However, if we compute the pdf of $\mathcal{A}$ under H_0, experimentally, we can observe a striking similarity between the experimental estimates, computed using normal EEG data, and the theoretical quantities derived from the aforementioned assumptions.

IV. Experimental Computation of the Power of the Statistical Test

In the previous sections, we developed a statistical test for the detection of ssVEP's. The *probability of detection* or *power* of the statistical test is the probability that the detection statistic $\mathcal{A}$ is greater than the threshold T_α, which corresponds to the *false-alarm* probability, α.

In this section, we experimentally compute the power of the statistical test (13), as a function of the signal-to-noise ratio (SNR). With SNR we mean

$$\text{SNR} = 10 \log \frac{\text{Power (VEP)}}{\text{Power (Post-stimulus EEG)}}. \qquad (21)$$

Analytical computation of the power of the test, for the finite sample case seems very complicated.

Experimental computation of the power of the test for given m, N and SNR, can be done as follows. We fix the false-alarm

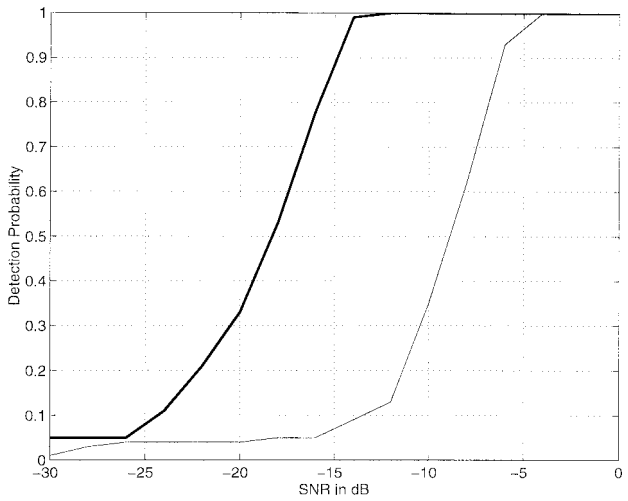

Fig. 2. Power of the periodogram-based (thick) and energy (thin) detectors with white Gaussian background noise; $m = 4$, $N = 1000$, false-alarm probability $\alpha = 0.01$.

probability α. This means that we can determine the threshold T_α

$$\Pr\left(\mathcal{A} > T_\alpha | H_0\right) = \alpha \tag{22}$$

from tables for the F-distribution. Then, for a given SNR we compute the probability that $\mathcal{A}$ exceeds T_α, by performing 500 realizations of the following experiment:

We generate $2N$ samples of pure EEG data (N prestimulus and N post-stimulus samples). This can be done in various ways; for example, we may use recorded EEG data, or we may generate artificial EEG's using AR models (using the MATLAB System Identification Toolbox [8] we observed that EEG data can be well modeled by AR models, with orders varying from 10 to 50).

Then, we generate N samples artificial VEP, as a sum of m harmonically related sinusoids. In order to obtain the desired SNR, we scale the VEP signal.

We form our test signal by adding the VEP to the post-stimulus EEG. Then we construct the test statistic $\mathcal{A}$ and we compare it with T_α. In this way we may compute the probability that for given m, N and SNR, $\mathcal{A}$ is greater than T_α, which is the power of the test.

In Fig. 1, we plot the power of the test as a function of the SNR, for $m = 4$, $N = 1000$, and false-alarm probability $\alpha = 0.01, 0.05$. We observe that our test has significant power for SNR higher than -18 dB.

If we wish to detect the presence of the signal without using any *a priori* knowledge about its properties, a reasonable choice appears to be the energy detector. Energy detection relies on the signal power only, and does not attempt to make use of any possible properties of the signal. Thus, comparing the performance of the periodogram-based and the energy detectors, will serve to illustrate the effect of utilizing the property (6) on the performance of the detection.

If we assume that the background noise in stationary white Gaussian with unknown variance, then the statistical test for

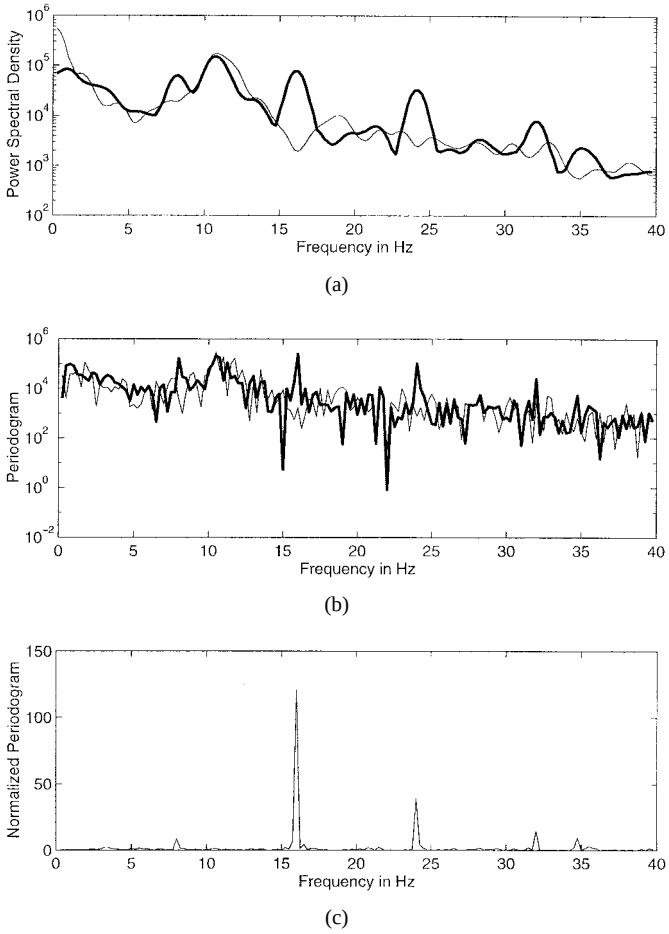

Fig. 3. Central Stimulation: (a) Power spectral densities for prestimulus (thin) and post-stimulus (thick) data, (b) periodograms for prestimulus (thin) and post-stimulus (thick) data, and (c) normalized post-stimulus periodogram $\boldsymbol{I}_{x\mathrm{post}}(\omega_k)/S_{y\mathrm{pre}}(\omega_k)$.

the energy detector is

$$\mathcal{B} = \frac{\sum_{n=1}^{N} y_{\mathrm{post}}^2(n)}{\sum_{n=1}^{N} y_{\mathrm{pre}}^2(n)} \tag{23}$$

which, under H_0, is distributed according to the $F(N, N)$ distribution. In Fig. 2, we plot the power of the statistical tests (13) and (23) for $m = 4$, $N = 1000$; the false-alarm probability α was set to 0.01. We observe that the periodogram-based detector takes advantage of *a priori* knowledge of the shape of the signal and performs much better than the simple energy detector.

V. Experimental Results

In this section, we will apply the statistical test for the detection of ssVEP's to real data.

We begin by presenting the results derived from central stimulation. We test for the presence of a periodic component composed of sinusoidal terms with frequencies 8, 16, 24,

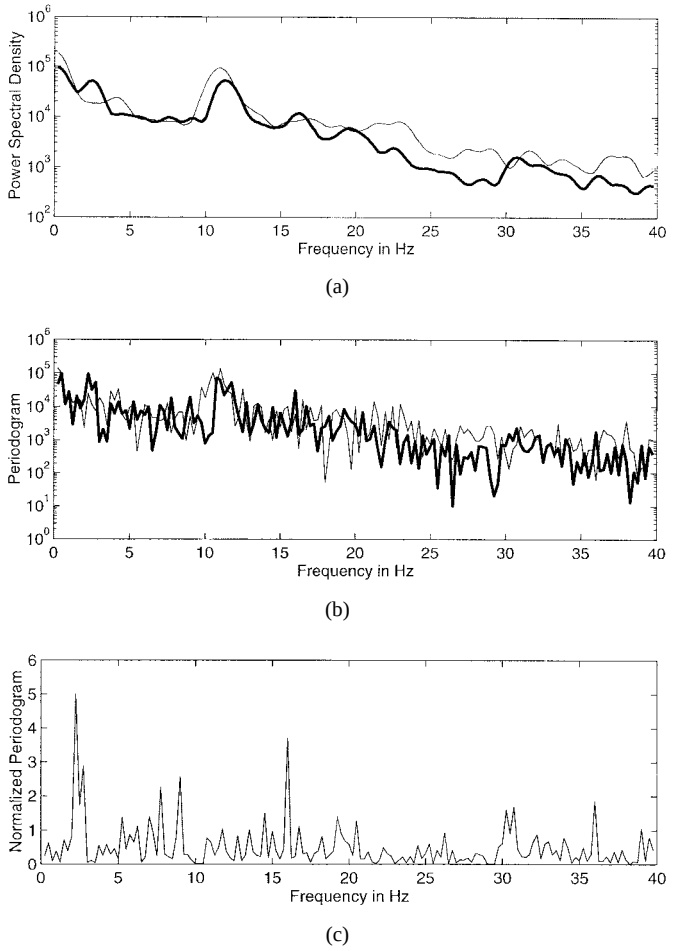

Fig. 4. Peripheral Stimulation: (a) Power spectral densities for prestimulus (thin) and post-stimulus (thick) data, (b) periodograms for prestimulus (thin) and post-stimulus (thick) data, and (c) normalized post-stimulus periodogram $\boldsymbol{I}_{x\mathrm{post}}(\omega_k)/S_{y\mathrm{pre}}(\omega_k)$.

and 32 Hz; we construct Ω using the frequency bins in the frequency range 0–40 Hz. In Fig. 3(a), we plot the psd's of the pre- and post-stimulus data with thin and thick lines, respectively, computed by means of the smoothed periodogram described in Section III. In Fig. 3(b), we plot the respective periodograms, while in Fig. 3(c), we plot the sequence $\boldsymbol{I}_{x\mathrm{post}}(\omega_k)/S_{y\mathrm{pre}}(\omega_k)$. We may form a first impression for the existence of the superimposed periodic component in the post-stimulus data, by just observing the psd's of the pre- and post-stimulus data. The existence of spectral peaks in the psd of the post-stimulus data at the harmonics of 8 Hz is obvious. Observing the "normalized" or "prewhitened" post-stimulus periodogram in Fig. 3(c), we can see very large peaks at the harmonics of 8 Hz, which take values of the order of 100. The test statistic for this example is $\mathcal{A} = 58.35$, which means that with probability (essentially) 1 it is not $F(8, 320)$-distributed. Consequently, we reject H_0 in favor of H_1.

When we move to the periphery of the eye the SNR becomes lower. In other words, we do not have strong sinusoidal components at all harmonics. We present such a case in Fig. 4. The main observation in Fig. 4(c) is that the peaks at the harmonics are not as strong as the corresponding peaks derived from central stimulation. In fact, there exist strong peaks due to EEG nonstationarities at the frequency ranges 2–4 Hz and around 30 Hz. However, since $\mathcal{A} = 2.5136$, we reject H_0 in favor of H_1 at level 0.0123.

We conclude this section by summarizing the results obtained from the application of our test on 20 data sets, derived from the inner area of the eye of healthy persons; in all these cases we detected stimulation response at level 0.015.

VI. Conclusion

In this paper, we developed a new ssVEP detection method. The method is based on the periodogram of a time-series. We test the post-stimulus data for the presence of hidden periodic components, which correspond to ssVEP's. We actually try to prewhiten the post-stimulus data, using the pre-stimulus data. In this way we obtain an expression of the change of the frequency contents of the signal between the pre- and post-stimulus parts.

Detection of periodic components actually means that there exists larger mean increase (smaller mean decrease) of the post-stimulus over the prestimulus psd's, at the harmonics of the basic stimulation frequency, compared to the corresponding mean increase (decrease) at the neighboring frequencies.

We experimentally computed the power of the statistical test. The periodogram-based detector takes advantage of the *a priori* knowledge of the signal shape and performs much better than the simple energy detector.

From the application of the method to real data we deduced that averaging over 32 realizations gives an SNR which is sufficient for detection with a very small false-alarm probability.

References

[1] D. Regan, *Human Brain Electrophysiology—Evoked Potentials and Evoked Magnetic Fields in Science and Medicine.* New York: Elsevier, 1989.
[2] F. Coelho, D. Simpson, and A. Infantosi, "Testing recruitment in the EEG under repetitive photo stimulation using frequency-domain approaches," in *Proc. IEEE Engineering in Medicine and Biology*, 1995.
[3] C. Davila, R. Srebro, and I. Ghaleb, "Objective measurement of visual contrast sensitivity via adaptive matched filtering of steady-state VEP's," in *Proc. IEEE Engineering in Medicine and Biology*, 1995.
[4] G. Henning, O. Hoenecke, P. Husar, K. Schellhorn, and U. Trautwein, "Time-frequency analysis of flicker-burst visual evoked responses," in *Proc. IEEE Engineering in Medicine and Biology*, 1995.
[5] P. Brockwell and R. Davis, *Time-Series: Theory and Methods.* New York: Springer-Verlag, 1991.
[6] L. Ljung, *System Identification—Theory for the User.* Englewood Cliffs, NJ: Prentice-Hall, 1987.
[7] A. Papoulis, *Probability and Statistics.* Englewood Cliffs, NJ: Prentice-Hall, 1990.
[8] L. Ljung, "MATLAB, System Identification Toolbox," 1987.

Athanasios P. Liavas was born in Pyrgos, Greece, in 1966. He received the diploma and the Ph.D. degree in computer engineering from the University of Patras, Greece, in 1989 and 1993, respectively.

From October 1993 to June 1995, he served in the Computer Center of the Greek Army. From August 1995 to April 1996, he worked as a Researcher in the Biomedical Engineering Department, Technical University of Ilmenau, Germany. Since June 1996, he has worked as a Researcher at the Institut National des Télécommunications, under the framework of the Training and Mobility of Researchers (T.M.R.) program of the European Commission. His research interests include adaptive signal processing algorithms, detection, and biomedical signal processing.

George V. Moustakides (S'79–M'83–SM'97) was born in Drama, Greece, in 1955. He received the diploma in electrical engineering from the National Technical University of Athens, Greece, in 1979; the M.Sc. degree in systems engineering from the Moore School of Electrical Engineering, University of Pennsylvania, Philadelphia, in 1980; and the Ph.D. degree in electrical engineering from Princeton University, Princeton, NJ, in 1983.

From 1983 to 1986, he held a Research Position at the Institut de Resherche en Informatique et Systemes Aleatoires (IRISA-INRIA), Rennes, France, and from 1987 to 1990, a Research Position at the Computer Technology Institute (CTI) of Patras, Patras, Greece. From 1991 to 1996, he was an Associate Professor in the Department of Computer Engineering and Informatics, University of Patras, and since 1996, he has been a Professor at the same department. His interests include adaptive signal processing algorithms, detection of signals, systems monitoring, and biomedical signal processing.

Günter Henning graduated from the Hochschule für Elektrotechnik Ilmenau, Germany, with the Dipl.-Ing. degree in 1965. He was a Research Assistant with Prof. Forth at the Department of Electromedical and Radiological Engineering in Ilmenau, from 1965 to 1974, and received a Dr.-Ing. degree in biomedical engineering in 1974.

He is a Professor at the Department of Biomedical Engineering and Medical Informatics, Technical University of Ilmenau. From 1974 to 1980, he was a Senior Researcher at the Medical Academy in Erfurt, Germany. Since 1980, he has been with the Technische Hoscschule Ilmenau. His current interests include noninvasive measurement of physiological parameters, electroophthalmologic diagnostic methods, and medical expert systems.

Emanouil Psarakis was born in Crete, Greece, in 1963. He received the Diploma degree in physics and the Ph.D. degree in computer engineering and informatics from the University of Patras, Greece, in 1985 and 1990, respectively.

Since 1993, he has been with the Computer Technology Institute (CTI) of Patras. His research interests include design and implementation of one-dimensional and multidimensional digital filters, voice and image compression, and signal processing algorithms for biomedical signals.

Peter Husar was born in Zilina, Slovakia, on September 18, 1956. He received the Dipl.-Ing. and Dr.-Ing. degrees in biomedical engineering from the Technical University of Ilmenau, Germany, in 1980 and 1986, respectively.

From 1986 to 1989, he was with the Research Institute for Computer Engineering in Zilina, Slovakia, and Siemens, Erlangen, Germany, as a Research Scientist in the field of medical image processing. From 1989 to 1992, he was employed at the University for Transport and Communication in Zilina as a Senior Researcher for signal processing and measurement technology. Since 1992, he has been with the Technical University of Ilmenau at the Institute for Biomedical Engineering and Medical Informatics, working in the field of objective perimetry and signal processing.